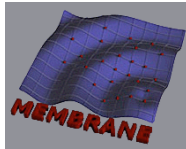


MEMBRANE

Deliverable D3.1



IST-4-027310 MEMBRANE

Deliverable D3.1

Capacity Analysis of MIMO Multi-hop Interference Relay Networks

Contractual Date of Delivery to the CEC:	September 30, 2006
Actual Date of Delivery to the CEC:	
Author(s):	C. Akçaba ¹ , V. Morgenshtern ¹ , H. Bölcskei ¹ , A. Alexiou ² and K. K. Leung ³
Participant(s):	ETHZ ¹ , Lucent ² , Imperial ³
Workpackage:	WP3.1
Est. person months:	13
Security:	Public
Nature:	R
Version:	0.2
Total number of pages:	29

Abstract:

In this deliverable, we develop a framework for evaluating different protocols (routing and scheduling) from an induced network (i.e. physical network in combination with protocol) capacity point of view. For MEMBRANE, such a framework is valuable in system design as it provides guidelines in distinguishing between different protocols in a concrete way. The effect of system parameters such as the number of relaying stages (hops) can be readily evaluated, decreasing the system design and testing time significantly.

Keyword list: MIMO, channel model, relay channel, multi-hop, physical layer performance, capacity, asymptotic analysis, interference, routing protocols.

I. INTRODUCTION

In this report, we develop a framework for evaluating different protocols (routing and scheduling) from an induced network (i.e. physical network in combination with protocol) capacity point of view. For MEMBRANE, such a framework is valuable in system design as it provides guidelines in distinguishing between different protocols in a concrete way. The effect of system parameters such as the number of relaying stages (hops) can be readily evaluated, decreasing the system design and testing time significantly.

In the next section, we provide an overview of the classical and the fading relay channels and their information theoretic treatment. In sections III to V, we analyze the different protocols for the single relay, fading channel case for non-regenerative (i.e. amplify-and-forward) and for regenerative (i.e. decode-and-forward) strategies. In section VI, we analyze multi-hop protocols for non-regenerative strategies. In the remainder of the report, we provide an asymptotic analysis for an interference relay network, where the effect of interference from other nodes, is also taken into account.

II. REVIEW OF FADING RELAY CHANNELS

We provide a brief literature review of the classical relay channel followed by a literature review of the fading relay channel.

A. Classical Relay Channel

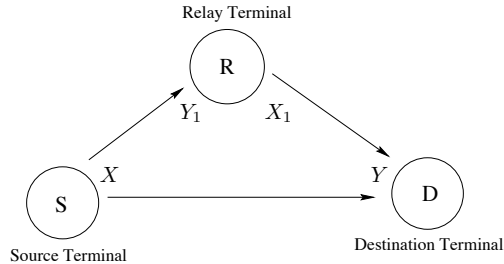


Fig. 1. Classical relay channel

The relay channel was introduced by van der Meulen [1] and recently attracted much interest from the research community due to the ready-applicability to wireless networks. The relay channel is depicted in 1, terminal S wishes to communicate with terminal D with the assistance of terminal R . The capacity of the relay channel is unknown except for special cases. Cover and El Gamal derived an upper-bound on relay channel capacity which can be interpreted as an application of maximum-flow minimum-cut theorem [2]:

$$C \leq \sup_{p(x, x_1)} \min \{I(X, X_1; Y), I(X; Y, Y_1|X_1)\} \quad (1)$$

Same authors also showed that the capacity of the physically degraded relay channel is given by:

$$C = \sup_{p(x, x_1)} \min\{I(X, X_1; Y), I(X; Y_1|X_1)\} \quad (2)$$

B. Example: Gaussian Relay Channel

The Gaussian relay channel is one of the few cases where channel capacity is known precisely. The Gaussian relay channel is an example of a physically degraded relay channel where terminal D has a degraded version of the signal observed at terminal R :

$$\begin{aligned} Y_1 &= X + Z_1 \\ Y &= X + Z_1 + X_1 + Z_2 \\ Z_i &\sim \mathcal{CN}(0, N_i) \end{aligned}$$

Cover and El Gamal derived the capacity of this channel [2]:

$$C = \max_{0 \leq \alpha \leq 1} \min \left\{ \log \left(1 + \frac{P + P_1 + 2\sqrt{(1-\alpha)PP_1}}{N_1 + N_2} \right), \log \left(1 + \frac{\alpha P}{N_1} \right) \right\} \quad (3)$$

where P and P_1 are power available at source and relay terminals respectively. The level of cooperation between source and relay terminal is controlled by variable α , such that α fraction of source power is used to convey new information to destination (and the relay) and $(1 - \alpha)$ fraction is used for resolving the ambiguity at the destination terminal.

Channels of interest are unfortunately not as easy to characterize as the Gaussian relay channel, and the exact capacity can seldom be calculated. For other classical results on the relay channel, please see references [1], [2]. Recent work on the relay channel focuses on wireless medium, and channel fading enters the picture. As opposed to characterizing the exact capacity of such channels, researchers have focused on ways of achieving distributed diversity, relaying methodologies and relay scheduling.

C. Fading Relay Channel

The wireless transmission medium is subject to random fluctuations of signal level in space, time and frequency caused by multipath nature of propagation and co-channel interference. Diversity is a way of combatting channel fading and improving link reliability. The classical way of achieving diversity is by supplying the receiver with multiple (ideally) independently fading replicas of the data signal in time, frequency or space. Appropriate combining at the receiver realizes diversity gain, thereby improving link reliability. Due to scarcity of resources such as bandwidth and time, it is often desirable to achieve diversity through spatial techniques (i.e. using additional antenna) in a communication system. Spatial diversity techniques have been extensively studied in the context of multiple-antenna systems [3]–[6].

Achieving diversity in a distributed fashion has been the focus of many works that enabled the interest in the subject to soar [7]–[10]. *Cooperative diversity* is achieved when nodes in

network cooperate to form a virtual antenna array realizing spatial diversity in a distributed fashion. Protocols for cooperation for channels with a single relay terminal have been analyzed in [11]–[14]. It has been shown that for channels with multiple relays, cooperative diversity with appropriately designed codes can achieve full spatial diversity gain [15]. Half-duplex relay channels were also studied in detail [16] [17]. In [16], a new protocol has been identified for the half-duplex single relay channel, which by maximizing the degree of collision and broadcast¹ achieves the diversity-multiplexing trade-off for amplify-and-forward based strategies. Diversity-Multiplexing tradeoffs have been derived for a variety of half-duplex relay channels in [17], and a new decode-and-forward based protocol that achieves the diversity-multiplexing trade-off (for certain multiplexing gains) for the single relay channel has been identified. For channels with multiple relays, Yang *et. al.* has shown that diversity-multiplexing curve achievable by a class of slotted amplify-and-forward protocols dominate diversity-multiplexing curves achievable by all other known AF-protocols [18]. Finally, we note that an array of works exists that study and analyze ways to achieve distributed beamforming in wireless networks [19]–[21] and that many cooperative diversity schemes can be cast into the framework of network coding [22]–[24].

III. THE SINGLE RELAY CASE

One of the key contributions of the work in [16] is the introduction of the induced channel model, which allows us to view the relay channel as a MIMO channel. This method allows us to analyze different relaying protocols using the tools developed for MIMO systems (e.g. DM trade-offs, code design criteria).

A. Problem setup

All terminals are equipped with single antenna transmitters and receivers. We impose half-duplex constraint on the relay terminals, hence terminals cannot receive and send information at the same time. The relay terminal either amplifies-and-forwards (AF) or decodes-and-forwards (DF) the received signal. The AF mode is non-regenerative in the sense that the relay terminal re-transmits the signal received from the source terminal after appropriate scaling (without reducing added noise). The DF mode is regenerative in the sense that the relay terminal demodulates and decodes prior to retransmission. AF mode relays require less complicated hardware compared to DF mode relays.

Regardless of the operation performed by the relay, we can schedule relay and source transmissions in a variety of ways. We define each such way as a protocol. Three protocols that were compared in [16] were:

Protocol I: The source terminal communicates with the relay and destination terminals during the first time slot. In the second time slot both the relay and source terminals communicate with the destination terminal. This protocol realizes maximum degrees of broadcasting and receive collision.

¹The degree of broadcasting is determined by the number of nodes listening to a broadcasted message.

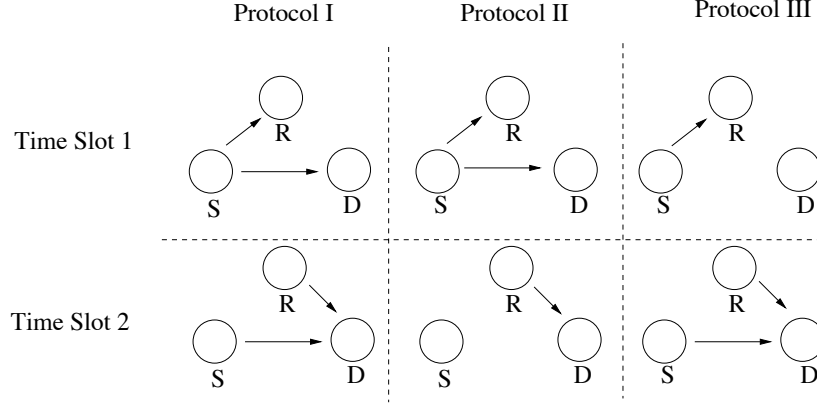


Fig. 2. Depiction of protocols

Protocol II: In this protocol the source terminal communicates with the relay and destination terminals over the first time slot. In the second time slot, only the relay terminal communicates with the destination terminal. This protocol realizes a maximum degree of broadcasting and exhibits no receive collision.

Protocol III: The third protocol is identical to Protocol I apart from the fact that the destination terminal chooses not to receive the direct² S→D signal during the first time slot for reasons that will be motivated later in this section. This protocol does not implement broadcasting but realizes receive collision.

Figure 2 summarizes the protocols.

B. Channel and Signal Models

Throughout this paper, we assume frequency-flat fading, no channel knowledge in the transmitters, perfect channel state information in the receivers and perfect synchronization.

Input-output relation for Protocol I in the AF mode. x_1 and x_2 denote the symbols transmitted in the first and second time slots, respectively. We assume that the symbols are zero-mean with unit-variance. The signal received at the destination terminal in the first time slot is given by

$$y_{D,1} = \sqrt{E_{SD}} h_{SD} x_1 + n_{D,1}, \quad (4)$$

The signal received at the relay terminal during the first time slot is given by

$$y_{R,1} = \sqrt{E_{SR}} h_{SR} x_1 + n_{R,1}, \quad (5)$$

where E_{XY} is the average signal energy received at the destination terminal over one symbol period through the X→Y link, h_{XY} is the random, complex-valued, unit-power channel gain between terminals X and Y and $n_{Y,i} \sim \mathcal{CN}(0, N_o)$ is additive white noise.

²A→B signifies the link between terminals A and B.

The relay terminal normalizes the received signal by a factor of $\sqrt{\mathcal{E}\{|y_{R,1}|^2\}}$ (so that the average energy is unity) and retransmits the signal during the second time slot. The destination terminal receives a superposition of the relay transmission and the source transmission during the second time slot according to

$$y_{D,2} = \sqrt{E_{SD}} h_{SD} x_2 + \sqrt{\frac{E_{SR}E_{RD}}{E_{SR} + N_o}} h_{SR} h_{RD} x_1 + \tilde{n}, \quad (6)$$

where the effective noise term $\tilde{n}|h_{RD} \sim \mathcal{CN}(0, N'_o)$ with $N'_o = N_o (1 + (E_{RD}|h_{RD}|^2)/(E_{SR} + N_o))$. Finally, we assume that the receiver normalizes $y_{D,2}$ by a factor³ $\omega = (1 + (E_{RD}|h_{RD}|^2)/(E_{SR} + N_o))^{1/2}$. This normalization does not alter the signal-to-noise ratio (SNR) but simplifies the ensuing presentation. The effective input-output relation for Protocol I in the AF mode can now be summarized as⁴

$$\mathbf{y}_1 = \mathbf{H}\mathbf{x} + \mathbf{n}, \quad (7)$$

where $\mathbf{y}_1 = [y_{D,1} \ y_{D,2}/\omega]^T$ is the received signal vector, \mathbf{H} is the effective 2×2 channel matrix given by

$$\mathbf{H} = \begin{bmatrix} \sqrt{E_{SD}} h_{SD} & 0 \\ \frac{1}{\omega} \sqrt{\frac{E_{SR}E_{RD}}{E_{SR} + N_o}} h_{SR} h_{RD} & \frac{\sqrt{E_{SD}}}{\omega} h_{SD} \end{bmatrix}, \quad (8)$$

$\mathbf{x} = [x_1 \ x_2]^T$ is the transmitted signal vector, and \mathbf{n} (when conditioned on the channel \mathbf{H}) is circularly symmetric complex Gaussian noise with $\mathcal{E}\{\mathbf{n}|\mathbf{H}\} = \mathbf{0}$ and $\mathcal{E}\{\mathbf{nn}^H|\mathbf{H}\} = N_o\mathbf{I}_2$. We shall make use of the fact that \mathbf{n} conditioned on \mathbf{H} is Gaussian when calculating the mutual information for the AF-based protocols in Section III.

Input-output relation for Protocol I in the DF mode. In the DF mode, still assuming Protocol I, the signal received at the destination terminal during the first time slot is identical to that for the AF mode and is hence given by (4). The signal received at the relay terminal is given by (5). Unlike the AF mode, the relay terminal now demodulates and decodes the signal received during the first time slot. Assuming that the signal is decoded correctly and retransmitted, we obtain

$$y_{D,2} = \sqrt{E_{SD}} h_{SD} x_2 + \sqrt{E_{RD}} h_{RD} x_1 + n_{D,2}.$$

The effective input-output relation in the DF mode for Protocol I can be summarized as

$$\mathbf{y}_1 = \mathbf{H}\mathbf{x} + \mathbf{n}, \quad (9)$$

where $\mathbf{y}_1 = [y_{D,1} \ y_{D,2}]^T$ is the received signal vector, \mathbf{H} is the effective 2×2 channel matrix given by

$$\mathbf{H} = \begin{bmatrix} \sqrt{E_{SD}} h_{SD} & 0 \\ \sqrt{E_{RD}} h_{RD} & \sqrt{E_{SD}} h_{SD} \end{bmatrix}, \quad (10)$$

³Recall that we assumed perfect channel state information in the receiver.

⁴The subscript 1 in \mathbf{y}_1 reflects the fact that we are dealing with Protocol I.

$\mathbf{x} = [x_1 \ x_2]^T$ is the transmitted signal vector, and \mathbf{n} is additive white Gaussian noise with $\mathcal{E}\{\mathbf{n}\} = \mathbf{0}$ and $\mathcal{E}\{\mathbf{nn}^H\} = N_o\mathbf{I}_2$. From (10) it is clear that knowledge of h_{SR} is not required at the destination terminal in the DF mode.

Input-output relation for Protocols II and III. The corresponding input-output relations for Protocols II and III in the AF and DF modes may be derived from (7) and (9), respectively. For Protocol II, the received signal for either forwarding mode can be written as

$$\mathbf{y}_2 = \mathbf{h}x_1 + \mathbf{n}, \quad (11)$$

where \mathbf{h} denotes the first column of \mathbf{H} (chosen appropriately from (8) or (10) depending on the transmission mode) and \mathbf{n} (conditioned on \mathbf{h} in the AF mode) is the 2×1 additive white complex Gaussian noise vector with $\mathcal{E}\{\mathbf{n}|\mathbf{h}\} = \mathbf{0}$ and $\mathcal{E}\{\mathbf{nn}^H|\mathbf{h}\} = N_o\mathbf{I}_2$. Similarly, the signal received at the destination terminal under Protocol III (the received signal is scalar in this case) satisfies

$$y_3 = \mathbf{g}^T \mathbf{x} + n, \quad (12)$$

where \mathbf{g}^T is the second row of \mathbf{H} (chosen appropriately from (8) or (10) depending on the transmission mode) and n (conditioned on \mathbf{g} in the AF mode) is scalar $\mathcal{CN}(0, N_o)$ additive white noise.

Note that the different protocols convert the spatially distributed antenna system into effective SIMO (with Protocol II), MISO (with Protocol III), and MIMO (with Protocol I) channels allowing the fundamental gains of multiple-antenna systems such as *diversity gain*, *array gain* and *interference canceling gain* to be exploited in a distributed fashion. We emphasize that *multiplexing gain* (i.e., a linear increase in achievable rate with the number of antennas in MIMO channels [25]–[28]) is conspicuously absent, since time is expended to create a virtual MIMO channel thereby negating any multiplexing gain. Further, note that the general structure and statistics of the effective channels created by the different protocols is different from the classical i.i.d. circularly symmetric complex Gaussian behavior widely used in the MIMO literature [4], [26], [27].

IV. INFORMATION-THEORETIC PERFORMANCE OF PROTOCOLS IN THE AF MODE

In this section, we analyze the information-theoretic performance of the three different AF-based protocols introduced in Section II.

A. Mutual Information of AF-Based Protocols

In the following, we employ an ergodic block-fading channel model (with independent blocks) and assume an i.i.d. Gaussian codebook with covariance matrix $\mathbf{R}_{\mathbf{xx}} = \mathcal{E}\{\mathbf{xx}^H\} = \mathbf{I}_2$. Moreover, we assume that the destination terminal has perfect knowledge of h_{SD} , h_{SR} and h_{RD} . The mutual information for Protocols I-III is obtained from (7), (11) and (12) as⁵

$$I_j^{AF} = \frac{1}{2} \log_2 \det \left(\mathbf{I}_2 + \frac{1}{N_o} \mathbf{A}_j^H \mathbf{A}_j \right) \text{ bps/Hz}, \quad j = 1, 2, 3, \quad (13)$$

⁵Recall that the noise is conditionally (on the channel) Gaussian.

where $\mathbf{A}_1 = \mathbf{H}$, $\mathbf{A}_2 = \mathbf{h}$, $\mathbf{A}_3 = \mathbf{g}$ and the factor $1/2$ accounts for the fact that information is conveyed to the destination terminal over two time slots. If coding is performed over an infinite number of independent channel realizations, the capacity of each of the three protocols, C_j^{AF} ($j = 1, 2, 3$), is given by the ergodic capacity $C_j^{AF} = \mathcal{E}\{I_j^{AF}\}$ with the expectation carried out with respect to the random channel. We emphasize that C_j^{AF} is the capacity of the single-relay fading channel *in conjunction* with Protocol j . If coding is performed only within one block the Shannon capacity is zero. In this case we resort to the $p\%$ outage capacity [29], [30], $C_{j,p,out}^{AF}$ ($j = 1, 2, 3$), defined as

$$P(I_j^{AF} \leq C_{j,p,out}^{AF}) = p\%, \quad (14)$$

or equivalently, the rate $C_{j,p,out}^{AF}$ is guaranteed to be supported for $(100 - p)\%$ of the channel realizations. In the following, we compare the different protocols in the AF mode both from a capacity (ergodic and outage) and a diversity point-of-view.

B. Comparison from a Capacity Point-of-View

It is been shown in [16] that :

$$I_1^{AF} > I_2^{AF} > I_3^{AF}$$

Since Protocol I offers maximum degree of broadcasting and receive collision, it does not suffer a loss in spectral efficiency. The source terminal is transmitting all the time in Protocol I, compared to other protocols and this explains the inferiority of other protocols which suffer from a factor of $1/2$ reduction in multiplexing gain (due to the source terminal being silent in the one time slot).

Finally, the fact that Protocol II is superior to Protocol III can be attributed to the fact that Protocol II corresponds to a SIMO system realizing array gain whereas Protocol III corresponds to a MISO system devoid of array gain (recall that we assumed perfect channel knowledge in the receivers and no channel knowledge in the transmitters). Maximizing the degree of broadcasting and receive collision (as is done in Protocol I) will in general result in a higher number of degrees-of-freedom (and hence higher achievable rates in the degrees-of-freedom limited case) reflected by the creation of an effective MIMO channel.

C. Diversity Performance

Comparing Protocols I-III in terms of diversity gain (as defined in [31]) we see that all protocols provide a second order gain, however the outage probabilities are ordered in the following fashion:

$$P(I_1^{AF} \leq C_{1,p,out}) < P(I_2^{AF} \leq C_{2,p,out}) < P(I_3^{AF} \leq C_{3,p,out})$$

V. INFORMATION-THEORETIC PERFORMANCE OF PROTOCOLS IN THE DF MODE

A. Comparison from a Capacity Point-of-View

It has been shown in [16] that the mutual information for the three protocols satisfies

$$I_1^{DF} \geq I_3^{DF} \geq I_2^{DF}. \quad (15)$$

under certain conditions on the distribution of power on transmit terminals. Consequently, the relation between the ergodic and outage capacities follows the same ordering. Again, the superiority of Protocol I can be attributed to the fact that it realizes multiplexing gain in the classical sense and hence recovers from some of the loss due to the use of two time slots for transmission⁶.

B. Comparison from a Diversity Point-of-View

Azarian *et. al.* has shown that Protocol I only offers first order diversity gain in DF mode [17]. This can be attributed to the fact that the relay terminal is forced to decode the source message after the first time slot. This is error prone as an error made by the relay terminal will be transmitted. Relaxing this constraint results in what is called the *dynamic decode-and-forward* (DDF) protocol, which lets the relay terminal defer its transmission until it has decoded correctly [17]. Naturally, Protocols II and III also offer unit diversity gain. This again is due to constraining the relay terminal to make a premature decision.

VI. EXTENSIONS TO MULTI-HOP MULTI-ANTENNA COMMUNICATION SCENARIOS

A. Multi-hop Extensions

The induced channel model can be extended to include scenarios where there are many relays in the communication environment. One-way to capture the multi-hop behavior is to use the slotted amplify-forward model, in which each relay repeats the source transmission in a time slot assigned to itself. We assume that communication takes place in the same frequency band, and relays receive transmission from other relays as well. The induced channel model for this modification is straightforward to derive from equation (8), and a two-relay example is provided in equation (16)

$$\mathbf{H}_{AF} = \begin{bmatrix} \sqrt{E_{sd}} h_{sd} & 0 & 0 \\ \frac{1}{w_1} \sqrt{\frac{E_{sr_1} E_{r_1d}}{\zeta_1}} h_{s_1r_1} h_{r_1d} & \frac{\sqrt{E_{sd}}}{w_1} h_{sd} & 0 \\ \frac{1}{w_2} \sqrt{\frac{E_{sr_1} E_{r_1r_2} E_{r_2d}}{\zeta_2 \zeta_1}} h_{sr_1} h_{r_1r_2} h_{r_2d} & \frac{1}{w_2} \sqrt{\frac{E_{sr_2} E_{r_2d}}{\zeta_2}} h_{sr_2} h_{r_2d} & \frac{\sqrt{E_{sd}}}{w_2} h_{sd} \end{bmatrix} \quad (16)$$

⁶Note that again allowing a flexible allocation of transmit power across the two time slots can lead to an ordering which is different from (15)

where $\zeta_1 = (E_{\text{sr}_1} + N_o)$ and, for $j \geq 2$, $\zeta_j = (E_{\text{sr}_j} + E_{\text{r}_{j-1}\text{r}_j} + N_o)$ and where w_i is defined as:

$$w_i = \left(1 + \sum_{j=1}^i E_{\text{r}_i\text{d}} |h_{\text{r}_i\text{d}}|^2 \prod_{k=1}^{j-1} \frac{E_{\text{r}_{i-k}\text{r}_{i-k+1}} |h_{\text{r}_{i-k}\text{r}_{i-k+1}}|^2}{\zeta_{i-k}} \right)^{1/2}$$

For a K relay system, the effective channel matrix \mathbf{H}_{AF} will be $K + 1$ dimensional. We also would like point out that extension to multi-antenna terminals is relatively easy, with the lower-triangular matrix shown in equation (16) replaced by a block-lower triangular structure. Assuming Gaussian codebooks as before, the mutual information between source and destination is given by:

$$\mathbf{I}_{\text{AF}} = \frac{1}{K} \log \det(\mathbf{I} + \frac{1}{N_o} \mathbf{H}\mathbf{H}^\dagger) \quad (17)$$

B. High SNR Approximation

Under a high SNR assumption on all links, mutual information can be approximated:

$$\mathbf{I}_{\text{AF}} \approx \frac{1}{K} \log \det(\tilde{\mathbf{H}}\tilde{\mathbf{H}}^\dagger) + \frac{1}{K} \log \det(\Omega\Omega^\dagger) - \log N_o \quad (18)$$

$$(19)$$

where $\mathbf{H} = \Omega\tilde{\mathbf{H}}$ and $\Omega = \text{diag}(1, \frac{1}{\omega_1}, \dots, \frac{1}{\omega_K})$. Since Ω , $\tilde{\mathbf{H}}$ and $\tilde{\mathbf{H}}$ are all triangular, we can explicitly write out the determinants for (18):

$$\mathbf{I}_{\text{AF}} \approx \frac{1}{K} \log (E_{\text{sd}} |h_{\text{sd}}|^2)^K + \frac{1}{K} \log \prod_{j=1}^{K-1} \frac{1}{w_j^2} - \log N_o \quad (20)$$

$$(21)$$

Then by some straightforward manipulation we have:

$$\mathbf{I}_{\text{AF}} \approx \log E_{\text{sd}} + \mathcal{E} \{ \log |h_{\text{sd}}|^2 \} - \frac{1}{K} \sum_{j=1}^{K-1} \mathcal{E} \{ \log w_j^2 \} - \log N_o \quad (22)$$

This approximation shows that under high SNR assumption multi-hopping in conjunction with amplify and forward protocol is inferior to direct transmission without relay assistance. The penalty terms $\frac{1}{K} \sum_{j=1}^{K-1} \mathcal{E} \{ \log w_j^2 \}$ are due to the amplified noise at relays, and as more noise gets 'repeated' by more relays the performance degrades faster.

C. Example: Application to a Multi-hop Scenario

In this section, we describe a scenario where the induced channel model can be used practically to distinguish between different communication protocols. We assume that a node (source) is to communicate with another node (sink) over the area pictured in figure 3, with the assistance of other nodes (relay nodes) which are scattered over the area. The source node does not know the locations of the other nodes in the network, and hence cannot decide whether the relay nodes should be allowed to participate in the communication. The average signal to noise ratio observed at any node is a function of pathloss and shadowing as stated before. In this example, we ignore the effects of shadowing and use a pathloss model where the received signal strength is inversely proportional to some exponent α of the distance between two nodes:

$$E_{SD} \sim \left(\frac{d_0}{d_{SD}} \right)^\alpha \quad (23)$$

$$E_{SR} \sim \left(\frac{d_0}{d_{SR}} \right)^\alpha \quad (24)$$

$$E_{RD} \sim \left(\frac{d_0}{d_{RD}} \right)^\alpha \quad (25)$$

where d_0 is the reference distance after which the suggested model is valid, and d_{SD} , d_{SR} and d_{RD} are the distances between source and destination, source and relay and relay and destination nodes respectively (see figure 3). In this example, we assume that source is located at point $(1, 1)$ and destination is located at point $(-1, -1)$. Two relays are randomly scattered over the rectangular area defined by $\{1.5, 1.5\}, \{-1.5, -1.5\}, \{-1.5, 1.5\}, \{1.5, -1.5\}$. There can be protocols where relay 1 transmits before relay 2, and vice versa. Since we do not know a priori which protocol will perform better, we will have to analyze the capacities for both orderings of the relays. Further, we assume that each relay can be either in a 'on' state, where it participates in communication effort, or in an 'off' state where it ignores the source transmissions. This setting defines five different operation states for the network after taking duplicate operating states into account. In table I we summarize the possible operating states.

TABLE I
OPERATING STATES

Time slot / Operating State	1	2	3	4	5
1	empty	R_1	R_2	R_1	R_2
2	empty	R_2	R_1	empty	empty

For each of these five operating states, we calculate the induced ergodic channel capacities and 10% outage capacities in order to find the best operating protocol. Figures (4) and (5) show the outage capacities and ergodic capacities of protocols respectively against pathloss coefficient, α , ranging from 2 to 5. The transmit power of relay and source terminals are scaled so that the average received signal to noise ratio is 0 dB at any pathloss level.

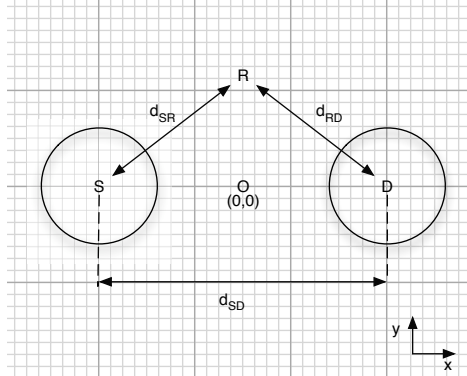


Fig. 3. Relative positions of terminals

In this example, relays are located at $(-0.7, 0.5)$ and $(0.2, 0.3)$. Due to the location of the relays we find that turning only relay 2 on (operating state 5) is favorable to other policies when ergodic capacity is the performance metric of interest. Likewise, turning both relays on with relay 2 transmitting before relay 1 (operating state 3) is favorable when outage capacity is the performance metric of interest.

This example demonstrates the convenience of the induced channel model in assessing the performance of different protocols. In this example, we had a 4-node network, but we had to enumerate five different operating states in order to decide the favorable policy. Even for such a small network, testing each configuration in real time is a tremendous overhead for the network operator. By eliminating some of the under-performing policies and configurations, the network operator or the designer can better utilize expensive resources such as real-time testing and can speed up on-site testing quite a bit. Although this example does not take into account the effects of shadowing, models that involve shadowing can be easily constructed and analyzed when needed. This example demonstrates how a MEMBRANE-like network can be analyzed from an induced capacity point of view and provide guidelines in system design. As there are other requirements in the MEMBRANE system such as delay requirements, the system design cannot be dependent entirely on the capacity analysis. Nevertheless, the tools developed provide a novel and valuable scheme to evaluate different protocols.

VII. ASYMPTOTIC ANALYSIS

A. General Assumptions

We consider an interference relay network (see Fig. 6) consisting of $K + 2M$ single-antenna terminals with M designated source-destination terminal pairs $\{\mathcal{S}_m, \mathcal{D}_m\}$ ($m \in [1:M]$) and K relays \mathcal{R}_k ($k \in [1:K]$). A dead-zone of nonzero radius around each \mathcal{S}_m and \mathcal{D}_m is free of relay terminals. We assume that no direct link between the individual source-destination terminal pairs exists (e.g., caused by large separation), transmission takes place in half-duplex fashion

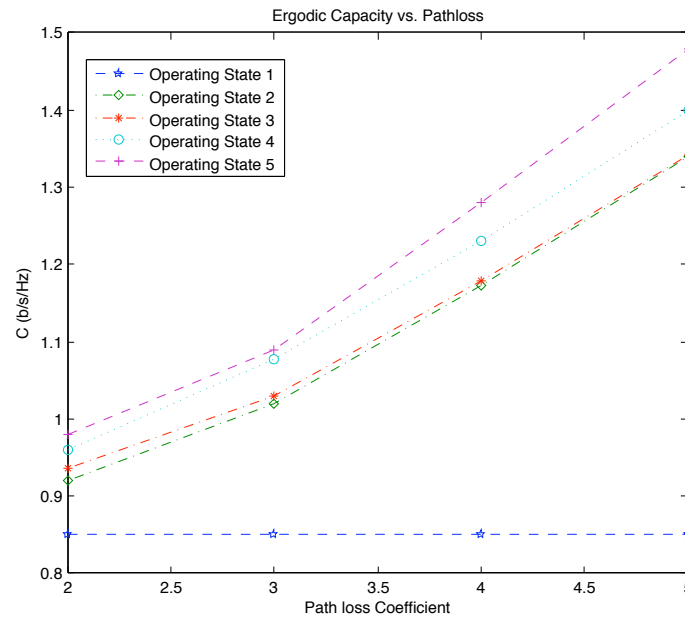


Fig. 4. Outage performance of different protocols

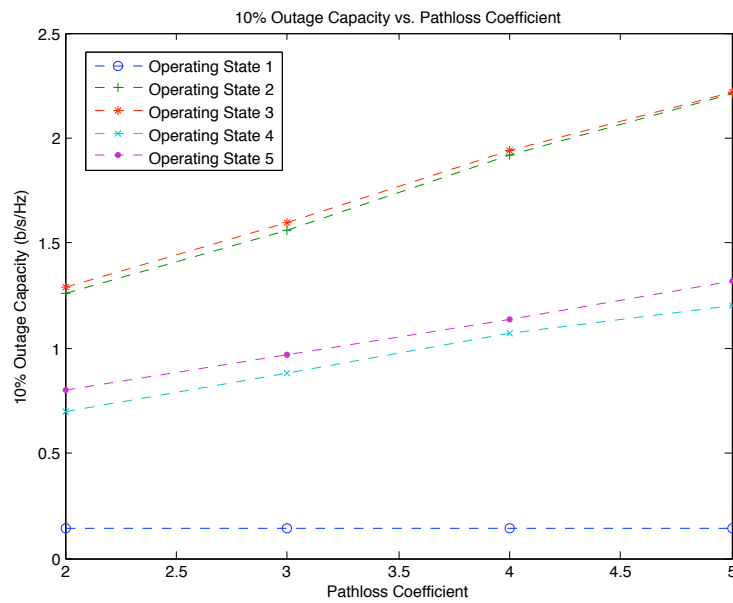


Fig. 5. Ergodic performance of different protocols

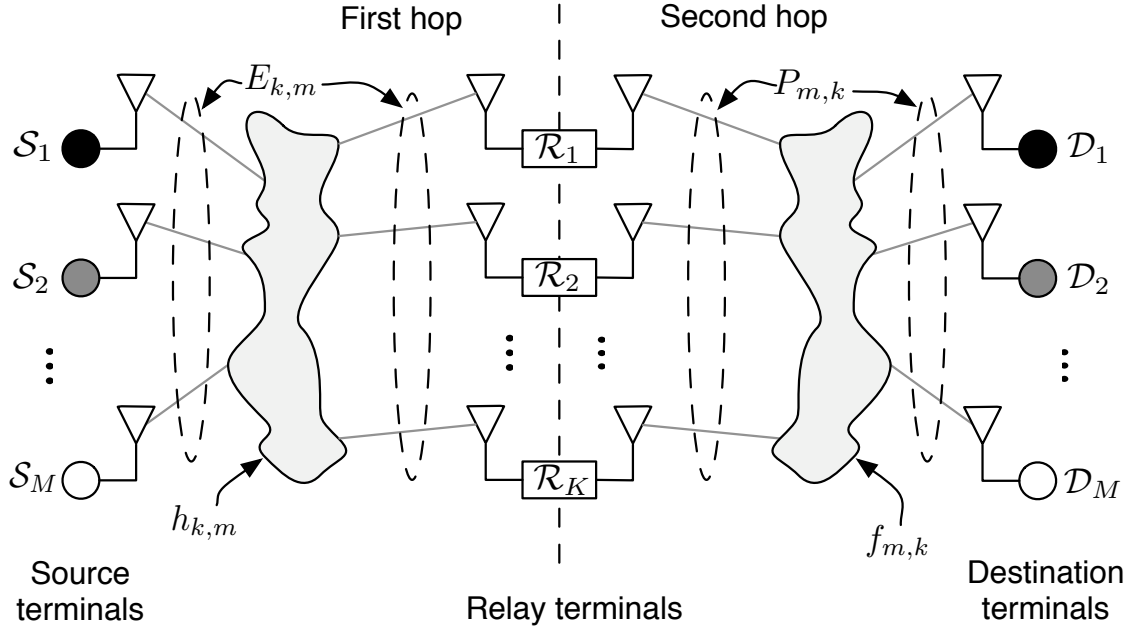


Fig. 6. Two-hop wireless relay network setup.

(the terminals cannot transmit and receive simultaneously) in two hops (a.k.a. two-hop relaying) over two separate time slots. In the first time slot the source terminals simultaneously broadcast their information to all the relay terminals (i.e., each relay terminal receives a superposition of all source signals). The relay terminals simultaneously broadcast (without additional processing) a scaled version of the signal to all the destination terminals during the second time slot. The source terminals do not have CSI. The destination terminals cooperate and perform joint decoding. Finally, we assume that all terminals are located within a domain of fixed area (dense network assumption). Our setup can be considered as an interference channel [32] with dedicated relays, hence the terminology *interference relay channel*.

B. Contributions and Relation to Previous Work

Previous work [33] demonstrated that for M fixed and $K \rightarrow \infty$, AF relaying turns the fading interference relay network into a fading point-to-point multiple-input multiple-output (MIMO) link, showing that the use of relays as active scatterers can recover spatial multiplexing gain in poor scattering environments. Our main contributions in this paper are as follows: The proof techniques in [33] rely heavily on M being finite. Building on results reported in [34], we compute the $M, K \rightarrow \infty$ (with $K/M \rightarrow \beta$ fixed) per source-destination terminal pair capacity using tools from large random matrix theory [35], [36]. The limiting eigenvalue density function of the effective MIMO channel matrix between the source and destination terminals is characterized in terms of its Stieltjes transform as the unique solution of a fixed-point equation,

which can be transformed into a fourth-order equation. Upon solving this fourth-order equation and applying the inverse Stieltjes transform, the remaining steps to computing the limiting eigenvalue density function and based on that the asymptotic network capacity have to be carried out numerically. We show that this can be accomplished in a straightforward fashion and provide a corresponding algorithm. We show that for $\beta \rightarrow \infty$, the fading AF relay network is turned into a fading point-to-point MIMO link thus establishing the large M, K analog of the result found previously for the finite- $M, K \rightarrow \infty$ case in [33].

C. Channel and Signal Model

Throughout the paper, frequency-flat fading over the bandwidth of interest and perfectly synchronized transmission/reception between the terminals is assumed. For the finite- $M, K \rightarrow \infty$ case it has been shown in [37] that the latter assumption can be relaxed, under quite general conditions on the synchronization errors, without impacting the capacity scaling laws. The input-output (I-O) relation for the link between the source terminals and the relay terminals during the first time slot is given by

$$\mathbf{r} = \mathbf{H}\mathbf{s} + \mathbf{z} \quad (26)$$

where $\mathbf{r} = [r_1, r_2, \dots, r_K]^T$ with r_k denoting the signal received at the k th relay terminal, $\mathbf{H} \in \mathbb{C}^{K \times M}$ with $[\mathbf{H}]_{k,m} = h_{k,m}$ ($k \in [1:K], m \in [1:M]$) where $h_{k,m} \sim \mathcal{CN}(0, 1)$ denotes the i.i.d. complex-valued channel gains corresponding to the $\mathcal{S}_m \rightarrow \mathcal{R}_k$ links, $\mathbf{s} = [s_1, s_2, \dots, s_M]^T$ where s_m is the zero-mean Gaussian signal transmitted by \mathcal{S}_m and the vector \mathbf{s} is temporally and spatially (across source terminals) i.i.d.. Finally, $\mathbf{z} = [z_1, z_2, \dots, z_K]^T$ where $z_k \sim \mathcal{CN}(0, \sigma^2)$ is temporally and spatially (across relay terminals) white noise. The k th relay terminal processes its received signal r_k to produce the output signal t_k . The collection of output signals t_k , organized in the vector $\mathbf{t} = [t_1, t_2, \dots, t_K]^T$ is then broadcast to the destination terminals during the second time slot while the source terminals are silent. The m th destination terminal receives the signal y_m with $\mathbf{y} = [y_1, y_2, \dots, y_M]^T$ given by

$$\mathbf{y} = \mathbf{F}\mathbf{t} + \mathbf{w} \quad (27)$$

where $\mathbf{F} \in \mathbb{C}^{M \times K}$ with $[\mathbf{F}]_{m,k} = f_{m,k}$ ($m \in [1:M], k \in [1:K]$) where $f_{m,k} \sim \mathcal{CN}(0, 1)$ denotes the i.i.d. complex-valued channel gains corresponding to the $\mathcal{R}_k \rightarrow \mathcal{D}_m$ links, and $\mathbf{w} = [w_1, w_2, \dots, w_M]^T$ with $w_m \sim \mathcal{CN}(0, \sigma^2)$ being temporally and spatially (across destination terminals) white noise. Throughout the paper, we impose a per-source-terminal power constraint $\mathbb{E}[|s_m|^2] \leq 1/M$ ($m \in [1:M]$), which results in the total transmit power trivially satisfying, $\mathbb{E}[\|\mathbf{s}\|^2] \leq 1$. Furthermore, we impose a per-relay-terminal power constraint $\mathbb{E}[|t_k|^2] \leq P_{\text{rel}}/K$ ($k \in [1:K]$), which results in the total power transmitted by the relay terminals satisfying $\mathbb{E}[\|\mathbf{t}\|^2] \leq P_{\text{rel}}$.

Throughout the paper, we assume that the source terminals \mathcal{S}_m ($m \in [1:M]$) do not have CSI. The assumptions on CSI at the relays and the destination terminals depend on the setup (coherent or noncoherent case) and the protocol (in the coherent case) and will be made specific when needed.

D. The AF Protocol

Upon reception of r_k , the k th relay terminal simply scales the received signal to obtain $t_k = (d/\sqrt{K}) r_k$. Choosing $d = \sqrt{P_{\text{rel}}/(1 + \sigma^2)}$ ensures that the per-relay power constraint $\mathbb{E}[\|\mathbf{t}_k\|^2] \leq P_{\text{rel}}/K$ and hence the total power constraint $\mathbb{E}[\|\mathbf{t}\|^2] \leq P_{\text{rel}}$ is met.

With these assumptions, inserting (26) into (27), we get the following I-O relation

$$\mathbf{y} = \frac{d}{\sqrt{K}} \mathbf{F} \mathbf{H} \mathbf{s} + \frac{d}{\sqrt{K}} \mathbf{F} \mathbf{z} + \mathbf{w}. \quad (28)$$

In the remainder of this section, we assume that the *jointly decoding destination terminals* have access to the realizations of \mathbf{H} and \mathbf{F} . In fact, as the analysis below shows, knowledge of $\mathbf{F} \mathbf{H}$ and \mathbf{F} is sufficient.

E. Capacity of the AF Protocol

Based on the I-O relation (28), we shall next study the behavior of $I(\mathbf{y}; \mathbf{s} | \mathbf{F} \mathbf{H}, \mathbf{F})$ when $M, K \rightarrow \infty$ with $K/M \rightarrow \beta$. We start by noting that

$$I(\mathbf{y}; \mathbf{s} | \mathbf{F} \mathbf{H}, \mathbf{F}) = \log \det \left(\mathbf{I} + \frac{d^2}{\sigma^2 M K} \mathbf{H}^H \mathbf{F}^H \left(\frac{d^2}{K} \mathbf{F} \mathbf{F}^H + \mathbf{I} \right)^{-1} \mathbf{F} \mathbf{H} \right).$$

Since the destination terminals perform joint decoding, the ergodic capacity per source-destination terminal pair is given by

$$C_{\text{AF}} = \frac{1}{2} \mathbb{E} \left[\frac{1}{M} \sum_{k=1}^K \log \left(1 + \frac{1}{\sigma^2} \lambda_k \left(\frac{1}{M} \mathbf{H} \mathbf{H}^H \mathbf{T} \right) \right) \right] \quad (29)$$

where

$$\mathbf{T} \triangleq \frac{d^2}{K} \mathbf{F}^H \left(\mathbf{I} + \frac{d^2}{K} \mathbf{F} \mathbf{F}^H \right)^{-1} \mathbf{F}$$

and the factor 1/2 in (29) results from the fact that data is transmitted over two time slots.

F. Asymptotic Capacity Behavior

To compute C_{AF} in the $M, K \rightarrow \infty$ limit with $K/M \rightarrow \beta$, we start by analyzing the corresponding asymptotic behavior⁷ of $\lambda_k((1/M) \mathbf{H} \mathbf{H}^H \mathbf{T})$. To this end, we define the Empirical Spectral Distribution (ESD) of a matrix (random or deterministic) according to

Definition 1: Let $\mathbf{X} \in \mathbb{C}^{N \times N}$ be a Hermitian matrix. The ESD of \mathbf{X} is defined as

$$F_{\mathbf{X}}^N(x) \triangleq \frac{1}{N} \sum_{n=1}^N I[\lambda_n(\mathbf{X}) \leq x].$$

⁷For a matrix X , $\lambda_k(X)$ denotes the k^{th} largest eigenvalue of X .

For random \mathbf{X} the quantity $F_{\mathbf{X}}^N(x)$ is random as well, i.e., it is a RV for each x . In the following, our goal is to prove the convergence (in the sense defined below), (when $M, K \rightarrow \infty$ with $K/M \rightarrow \beta$ and $\beta \in (0, \infty)$) of $F_{(1/M)\mathbf{H}\mathbf{H}^H\mathbf{T}}^K(x)$ to a deterministic limit and find the corresponding limiting eigenvalue distribution.

Definition 2: We say that the ESD $F_{\mathbf{X}}^N(x)$ of a random Hermitian matrix $\mathbf{X} \in \mathbb{C}^{N \times N}$ converges a.s. to a deterministic limiting function $F_{\mathbf{X}}(x)$, when $N \rightarrow \infty$, if for any $\epsilon > 0$ there exists an $N_0 > 0$ s.t. $\forall N \geq N_0$ a.s.

$$\sup_{x \in \mathbb{R}} |F_{\mathbf{X}}^N(x) - F_{\mathbf{X}}(x)| \leq \epsilon.$$

To prove the convergence of $F_{(1/M)\mathbf{H}\mathbf{H}^H\mathbf{T}}^K(x)$ to a deterministic limiting function, we start by analyzing $F_{\mathbf{T}}^K(x)$.

Lemma 1: For $M, K \rightarrow \infty$ with $K/M \rightarrow \beta$, the ESD $F_{\mathbf{T}}^K(x)$ converges a.s. to a nonrandom limiting distribution $F_{\mathbf{T}}(x)$ with corresponding density given by⁸

$$f_{\mathbf{T}}(x) = \frac{\sqrt{(1+\gamma_1)(1+\gamma_2)}}{2\pi d^2 x(1-x)^2} \sqrt{\left(\frac{\gamma_2}{1+\gamma_2} - x\right)^+ \left(x - \frac{\gamma_1}{1+\gamma_1}\right)^+} + \left[1 - \frac{1}{\beta}\right]^+ \delta(x) \quad (30)$$

where $\gamma_1 \triangleq d^2(1 - 1/\sqrt{\beta})^2$ and $\gamma_2 \triangleq d^2(1 + 1/\sqrt{\beta})^2$.

Proof: We start with the singular value decomposition

$$\frac{d}{\sqrt{K}}\mathbf{F} = \mathbf{U}\mathbf{\Sigma}\mathbf{V}$$

where the columns of $\mathbf{U} \in \mathbb{C}^{M,M}$ are the eigenvectors of the matrix $(d^2/K)\mathbf{F}\mathbf{F}^H$, the columns of $\mathbf{V}^H \in \mathbb{C}^{K,K}$ are the eigenvectors of $(d^2/K)\mathbf{F}^H\mathbf{F}$, the matrix $\mathbf{\Sigma} \in \mathbb{R}^{M,K}$ contains $R = \min(M, K)$ nonzero entries $\Sigma_{11}, \Sigma_{22}, \dots, \Sigma_{RR}$, which are the positive square roots of the nonzero eigenvalues of the matrix $(d^2/K)\mathbf{F}\mathbf{F}^H$. Defining $\mathbf{\Lambda} \triangleq \mathbf{\Sigma}\mathbf{\Sigma}^H \in \mathbb{R}^{M,M}$, we have

$$\mathbf{T} = \mathbf{V}^H\mathbf{\Sigma}^H(\mathbf{I} + \mathbf{\Lambda})^{-1}\mathbf{\Sigma}\mathbf{V}.$$

By inspection, it follows that

$$F_{\mathbf{\Sigma}^H(\mathbf{I}+\mathbf{\Lambda})^{-1}\mathbf{\Sigma}}^K(x) = \frac{M}{K}F_{\mathbf{\Lambda}}^M\left(\frac{x}{1-x}\right) + \left(1 - \frac{M}{K}\right)u(x). \quad (31)$$

As $F_{\mathbf{\Lambda}}^M(x) = F_{(d^2/K)\mathbf{F}\mathbf{F}^H}^M(x)$, by the Marčenko-Pastur law (see Theorem 2 in Appendix A), we conclude that $F_{\mathbf{\Lambda}}^M(x)$ converges a.s. to a limiting nonrandom distribution $F_{\mathbf{\Lambda}}(x)$ with corresponding density

$$f_{\mathbf{\Lambda}}(x) = \frac{\beta}{2\pi x d^2} \sqrt{(\gamma_2 - x)^+ (x - \gamma_1)^+} + [1 - \beta]^+ \delta(x). \quad (32)$$

⁸Note that (30) implies that $f_{\mathbf{T}}(x)$ is compactly supported in the interval $[\gamma_1/(1+\gamma_1), \gamma_2/(1+\gamma_2)]$.

From (31) we can therefore conclude that $F_{\Sigma^H(\mathbf{I}+\mathbf{\Lambda})}^K(x)$ converges a.s. to a nonrandom limit given by

$$F_{\Sigma^H(\mathbf{I}+\mathbf{\Lambda})}^{-1\Sigma}(x) = \frac{1}{\beta} F_{\mathbf{\Lambda}} \left(\frac{x}{1-x} \right) + \left(1 - \frac{1}{\beta} \right) u(x). \quad (33)$$

Taking the derivative w.r.t. x on both sides of (33), the density corresponding to $F_{\Sigma^H(\mathbf{I}+\mathbf{\Lambda})}^{-1\Sigma}(x)$ is obtained as

$$f_{\Sigma^H(\mathbf{I}+\mathbf{\Lambda})}^{-1\Sigma}(x) = \frac{1}{\beta} f_{\mathbf{\Lambda}} \left(\frac{x}{1-x} \right) \frac{1}{(1-x)^2} + \left(1 - \frac{1}{\beta} \right) \delta(x). \quad (34)$$

The final result in (30) now follows by noting that $f_{\mathbf{T}}(x) = f_{\Sigma^H(\mathbf{I}+\mathbf{\Lambda})}^{-1\Sigma}(x)$ due to the unitarity of \mathbf{V} and by inserting (32) into (34) and carrying out straightforward algebraic manipulations. \blacksquare

Based on Lemma 1, we can now apply Theorem 1 (Appendix A) to conclude that $F_{(1/M)\mathbf{H}\mathbf{H}^H\mathbf{T}}^K(x)$ converges a.s. to a deterministic function $F_{(1/M)\mathbf{H}\mathbf{H}^H\mathbf{T}}(x)$ as $M, K \rightarrow \infty$ with $K/M \rightarrow \beta$. The corresponding limiting density $f_{(1/M)\mathbf{H}\mathbf{H}^H\mathbf{T}}(x)$ is obtained by applying the Stieltjes inversion formula (47) to the solution of the fixed point equation

$$G(z) = \underbrace{\int_{-\infty}^{\infty} \frac{f_{\mathbf{T}}(x) dx}{x(1-\beta-\beta z G(z)) - z}}_I, \quad z \in \mathbb{C}^+ \quad (35)$$

in the set

$$\{G(z) \in \mathbb{C} \mid -(1-\beta)/z + \beta G(z) \in \mathbb{C}^+\}, \quad z \in \mathbb{C}^+ \quad (36)$$

where we used the symbol $G(z)$ to denote the Stieltjes transform $G_{(1/M)\mathbf{H}\mathbf{H}^H\mathbf{T}}(z)$. In the following, for brevity, we write G instead of $G(z)$. To solve (35), we first compute the integral I on the RHS of (35). Substituting $f_{\mathbf{T}}(x)$ from (30) into (35) and defining

$$\eta_1 \triangleq \frac{\gamma_1}{1+\gamma_1}, \quad \eta_2 \triangleq \frac{\gamma_2}{1+\gamma_2}, \quad \rho \triangleq \frac{\sqrt{(1+\gamma_1)(1+\gamma_2)}}{2\pi d^2}$$

we obtain

$$I = -\frac{1}{z} \left[1 - \frac{1}{\beta} \right]^+ + \frac{1}{z} \underbrace{\int_{\eta_1}^{\eta_2} \frac{\rho \sqrt{(\eta_2 - x)(x - \eta_1)} dx}{x(1-x)^2 \left[x \left(\frac{1-\beta}{z} - \beta G \right) - 1 \right]}}_{\hat{I}}. \quad (37)$$

The integral \hat{I} is computed in Appendix B. Employing the notation introduced in Appendix B, the fixed point equation (35) can finally be written as

$$Gz = - \left[1 - \frac{1}{\beta} \right]^+ + \chi A_1 \hat{I}_1 + \chi A_2 \hat{I}_2 + \chi A_3 \hat{I}_3 + \chi A_4 \hat{I}_4. \quad (38)$$

It is tedious, but straightforward, to show that for any $\beta > 0$

$$- \left[1 - \frac{1}{\beta} \right]^+ + \chi A_1 \hat{I}_1 = -\frac{\beta-1}{2\beta}$$

so that (38) can be written as

$$Gz + \frac{\beta - 1}{2\beta} - \chi A_2 \hat{I}_2 - \chi A_3 \hat{I}_3 = \chi A_4 \hat{I}_4. \quad (39)$$

Next, multiplying (39) by $2d^2\beta(G\beta z + z + \beta - 1)^2$, squaring both sides, introducing the auxiliary variable

$$\hat{G} \triangleq -\frac{1 - \beta}{z} + \beta G \quad (40)$$

it follows after straightforward, but tedious, manipulations that \hat{G} must satisfy the following quartic equation

$$\hat{G}^4 + a_3 \hat{G}^3 + a_2 \hat{G}^2 + a_1 \hat{G} + a_0 = 0 \quad (41)$$

with the coefficients

$$\begin{aligned} a_3 &= \frac{1}{z}(2z - \beta + 1) & a_2 &= \frac{1}{z} \left(z - \beta + 3 - \frac{\beta}{d^2} \right) \\ a_1 &= \frac{1}{z^2} \left(2z - \beta + 1 - \frac{\beta}{d^2} \right) & a_0 &= \frac{1}{z^2}. \end{aligned}$$

The quartic equation (41) can be solved analytically. The resulting expressions are, however, very lengthy, do not lead to interesting insights and will therefore be omitted. It is important to note, however, that (41) has two pairs of complex conjugate roots. The solutions of (41) will henceforth be denoted as $\hat{G}_1, \hat{G}_1^*, \hat{G}_2$, and \hat{G}_2^* . We recall that our goal is to find the unique solution G of the fixed point equation (35) s.t. $\hat{G} = -(1 - \beta)/z + \beta G \in \mathbb{C}^+ \forall z \in \mathbb{C}^+$. Therefore, in each point $z \in \mathbb{C}^+$ we can immediately eliminate the two solutions (out of the four) that have a negative imaginary part. In practice, this can be done conveniently by constructing the functions $\hat{G}'_1 \triangleq \Re \hat{G}_1 + j \Im \hat{G}_1$ and $\hat{G}'_2 \triangleq \Re \hat{G}_2 + j \Im \hat{G}_2$, which can be computed analytically, satisfy (41) and are in \mathbb{C}^+ for any $z \in \mathbb{C}^+$. Next, note that (39) has a unique solution in the set (36), which is also the unique solution of (35). This solution $G(z)$, $z \in \mathbb{C}^+$, can be obtained by simply substituting $G_1 = (1/\beta)(\hat{G}'_1 - (\beta - 1)/z)$ and $G_2 = (1/\beta)(\hat{G}'_2 - (\beta - 1)/z)$ into (39) and checking, which of the two satisfies the equation. Unfortunately, it seems that this verification cannot be formalized in the sense of identifying the unique solution of (39) in analytic form. The primary reason for this is that to check *algebraically* if G_1 and G_2 satisfy (39), we have to perform a noninvertible transformation (squaring) of (39), which doubles the number of solutions of this equation, and results in G_1 and G_2 both satisfying the resulting formula. The second reason is that depending on the values of the parameters $\beta > 0, d > 0$, the correct solution is either G_1 or G_2 and the dependence between G_1, G_2, β and d has a complicated structure. Starting from the analytical expressions for G_1 and G_2 , we can, however, for any fixed $\beta > 0, d > 0$, identify the density function $f_{(1/M)\mathbf{HH}^H\mathbf{T}}(x) = (1/\pi) \lim_{y \rightarrow 0^+} \Im[G(x + jy)]$ corresponding to the unique solution of (39) [and hence of (35)] numerically. This is accomplished as follows. We know that, for given x , $\lim_{y \rightarrow 0^+} \Im[G(x + jy)]$ is either equal to

$$L_1(x) \triangleq \lim_{y \rightarrow 0^+} \Im[G_1(x + jy)]$$

or

$$L_2(x) \triangleq \lim_{y \rightarrow 0^+} \Im[G_2(x + jy)].$$

Even though the functions $L_1(x)$ and $L_2(x)$ can be computed analytically (with the resulting expressions being very lengthy and involved), it seems that for any fixed $x > 0$ the correct choice between the values $L_1(x)$ and $L_2(x)$ can only be made numerically. The following algorithm constitutes one possibility to solve this problem.

Algorithm—Choice of the Limit

Input: $x > 0$

- 1) Choose a small enough $y > 0$
- 2) Substitute $G_1(x + jy)$ and $G_2(x + jy)$ into (39)
- 3) If $G_1(x + jy)$ satisfies (39), then
 return $L_1(x)$
 otherwise
 return $L_2(x)$

As any other numerical procedure, this algorithm includes an element of heuristics. The following comments are therefore in order.

- In Step 1) the choice of y cannot be formalized in the sense of giving an indication of how small it has to be as a function of β and d . On the one hand y has to be strictly greater than zero, because (39) in general holds in \mathbb{C}^+ only and does not need to hold neither for $G_1(x + j0)$ nor for $G_2(x + j0)$. On the other hand, y should be small enough for $G_1(x + jy)$ to be close to $L_1(x)$ and $G_2(x + jy)$ to be close to $L_2(x)$. The correctness of the output of the algorithm is justified by the analyticity (see Definition 3) of $G(z)$ in \mathbb{C}^+ .
- In Step 3) the check whether $G_1(x + jy)$ satisfies (39) is performed numerically. Therefore, rounding errors will arise. It turns out, however, that, in practice, unless $|L_1(x) - L_2(x)|$ is very small (in this case it does not matter which of the two values we choose), the solution of (39) yields a clear indication whether $G_1(x + jy)$ or $G_2(x + jy)$ is the correct choice.
- In order to compute the density $f_{(1/M)\mathbf{HH}^H\mathbf{T}}(x)$ using the proposed algorithm, we need to run Steps 1)-3) for every x . It will be proved below that $f_{(1/M)\mathbf{HH}^H\mathbf{T}}(x)$ is always compactly supported and bounds for its support will be given in analytic form (as a function of β and d). Since the algorithm consists of very basic arithmetic operations only, it is very fast and can easily be run on a dense grid inside the support region of $f_{(1/M)\mathbf{HH}^H\mathbf{T}}(x)$.

As an example, for $d = 1$ and $\beta = 1/2$, Fig. 7(a) shows the density $f_{(1/M)\mathbf{HH}^H\mathbf{T}}(x)$ obtained by the algorithm formulated above along with the histogram of the same density obtained through Monte-Carlo simulation. We can see that the two curves match very closely and that our method allows to obtain a much more refined picture of the limiting density. Fig. 7(b) shows the density $f_{(1/M)\mathbf{HH}^H\mathbf{T}}(x)$ for $\beta = 2, 1, 1/2$ obtained through our algorithm. We can see that the density function is always compactly supported.

The final step in computing the asymptotic capacity of the AF relay network is to take the limit $K, M \rightarrow \infty$ with $K/M \rightarrow \beta$ in (29) and evaluate the resulting integral

$$C_{\text{AF}}^\beta \triangleq \frac{\beta}{2} \int_0^\infty \log\left(1 + \frac{x}{\sigma^2}\right) f_{(1/M)\mathbf{H}\mathbf{H}^H\mathbf{T}}(x) dx \quad (42)$$

numerically. The evaluation of (42) is drastically simplified by recognizing that $f_{(1/M)\mathbf{H}\mathbf{H}^H\mathbf{T}}(x)$ is compactly supported. The corresponding interval boundaries (or, more specifically, bounds thereon) can be computed analytically as a function of β and d . We start by noting that the second part of Theorem 2 in Appendix A implies that a.s. $\lim_{M \rightarrow \infty} \lambda_{\max}((1/M)\mathbf{H}\mathbf{H}^H) = (1 + \sqrt{\beta})^2$. Based on (34) and using Theorem 2, it follows that a.s. $\lambda_{\max}(\mathbf{T}) = d^2(1 + \sqrt{\beta})^2/(\beta + d^2(1 + \sqrt{\beta})^2)$. For any realization of \mathbf{H} and \mathbf{T} and any M, K , by the submultiplicativity of the spectral norm, we have

$$\lambda_{\max}((1/M)\mathbf{H}\mathbf{H}^H\mathbf{T}) \leq \lambda_{\max}((1/M)\mathbf{H}\mathbf{H}^H) \lambda_{\max}(\mathbf{T})$$

which implies that for $M, K \rightarrow \infty$ with $K/M \rightarrow \beta$ a.s.

$$\lambda_{\max}((1/M)\mathbf{H}\mathbf{H}^H\mathbf{T}) \leq \frac{d^2(1 + \sqrt{\beta})^4}{\beta + d^2(1 + \sqrt{\beta})^2} \triangleq x_{\max}.$$

We can therefore conclude that $f_{(1/M)\mathbf{H}\mathbf{H}^H\mathbf{T}}(x)$ is compactly supported on the interval⁹ $[0, x_{\max}]$. Consequently, the integral in (42) becomes

$$C_{\text{AF}}^\beta = \frac{\beta}{2} \int_0^{x_{\max}} \log\left(1 + \frac{x}{\sigma^2}\right) f_{(1/M)\mathbf{H}\mathbf{H}^H\mathbf{T}}(x) dx$$

which can be computed numerically, using any standard method for numerical integration and employing the algorithm described above to evaluate $f_{(1/M)\mathbf{H}\mathbf{H}^H\mathbf{T}}(x)$ at the required grid points. Using this procedure, we computed C_{AF}^β as a function of β for $d = 1$ with the result depicted in Fig. 8. We can see that for $\beta < 1$ (i.e., $K < M$) C_{AF}^β increases very quickly with β , which is due to the fact that the corresponding effective MIMO channel matrix is building up rank and hence spatial multiplexing gain. For $\beta > 1$ (i.e., $K > M$), when the effective MIMO channel matrix is already full-rank with high probability, the curve flattens out and for $\beta \rightarrow \infty$, the capacity C_{AF}^β seems to converge to a finite value. In the next subsection, we prove that C_{AF}^β indeed converges to a finite limit as $\beta \rightarrow \infty$. This result has an interesting interpretation as it allows to relate the AF relay network to a point-to-point MIMO channel.

G. Convergence to Point-to-Point MIMO Channel

In [33] it was shown that for finite M as $K \rightarrow \infty$ the two-hop AF relay network capacity converges to half the capacity of a point-to-point MIMO link; the factor 1/2 penalty comes from the fact that communication takes place over two time slots. In the following, we demonstrate that the result in [33] can be generalized to the $M, K \rightarrow \infty$ case. More specifically, we show that for $\beta \rightarrow \infty$ the asymptotic ($M, K \rightarrow \infty$) capacity of the two-hop AF relay network is equal

⁹The actual supporting interval of $f_{(1/M)\mathbf{H}\mathbf{H}^H\mathbf{T}}(x)$ may, in fact, be smaller.

to half the asymptotic ($M \rightarrow \infty$) capacity of a point-to-point MIMO channel with M transmit and M receive antennas. We start by dividing (41) by β and taking the limit¹⁰ $\beta \rightarrow \infty$, which yields the quadratic equation

$$z\hat{G}^2 + z\left(1 + \frac{1}{d^2}\right)\hat{G} + \left(1 + \frac{1}{d^2}\right) = 0. \quad (43)$$

The two solutions of (43) are given by

$$\hat{G}_{1,2}(z) = \frac{-z\left(1 + \frac{1}{d^2}\right) \pm \sqrt{z^2\left(1 + \frac{1}{d^2}\right)^2 - 4z\left(1 + \frac{1}{d^2}\right)}}{2z}. \quad (44)$$

Applying the Stieltjes inversion formula (47) to (44) and choosing the solution, which yields a positive density function, we obtain

$$\begin{aligned} \beta f_{(1/M)\mathbf{H}\mathbf{H}^H\mathbf{T}}(x) &= \frac{1}{\pi} \lim_{y \rightarrow 0^+} \Im [\beta G(x + jy)] \\ &= \frac{1}{\pi} \lim_{y \rightarrow 0^+} \Im [\hat{G}(x + jy)] \\ &= \frac{1}{2\pi x} \sqrt{\left[4x\left(1 + \frac{1}{d^2}\right) - x^2\left(1 + \frac{1}{d^2}\right)^2\right]^+}. \end{aligned} \quad (45)$$

Inserting (45) into (42) and changing the integration variable according to $u \triangleq x(1 + 1/d^2)$, we find that

$$C_{\text{AF}}^{\beta} \xrightarrow{\beta \rightarrow \infty} C_{\text{AF}}^{\infty} \triangleq \frac{1}{4\pi} \int_0^4 \sqrt{\frac{4}{u} - 1} \log\left(1 + \frac{d^2}{(d^2 + 1)\sigma^2} u\right) du. \quad (46)$$

Comparing (46) with [38, Eq. (13)], it follows that for $\beta \rightarrow \infty$ the asymptotic $M, K \rightarrow \infty$ with $K/M \rightarrow \beta$ per source-destination terminal pair capacity in the two-hop AF relay network is equal to half the asymptotic ($M \rightarrow \infty$) per-antenna capacity in a point-to-point MIMO link with M transmit and M receive antennas, provided the SNR in the relay case is defined as $\text{SNR} \triangleq d^2 / ((d^2 + 1)\sigma^2)$. For M and K large, it is easy to verify that this choice corresponds to the SNR at each destination terminal in the AF relay network. In this sense, we can conclude that for $\beta \rightarrow \infty$ the AF relay network “converges” to a point-to-point MIMO link with the same received SNR.

VIII. CONCLUSION

For single relay fading channels, we evaluated all possible cooperation protocols, providing information theoretic comparisons in terms of diversity and multiplexing. Protocols with high degree of receive collision seem to perform better than protocols with a lower degree of receive collision. For the amplify-and-forward strategy, we extended our analysis to multi-hop relay

¹⁰It is important that first we take the limit $M, K \rightarrow \infty$ with $K/M \rightarrow \beta$ and afterwards let $\beta \rightarrow \infty$.

networks, and showed that at high-SNR there is a drop in the capacity that can be associated with high amplification of noise at relay terminals. The techniques and tools we developed for the analysis of such networks can be augmented with pathloss and shadowing models in the context of MEMBRANE to provide guidelines in system design.

For noncoherent fading interference relay networks with amplify-and-forward relaying and joint decoding at the cooperating destination terminals, we computed the asymptotic (in M and K with $K/M \rightarrow \beta$ fixed) network capacity using tools from large random matrix theory. To the best of our knowledge, this is the first application of large random matrix theory to characterize the capacity behavior of large fading networks. We furthermore demonstrated that for $\beta \rightarrow \infty$ the relay network converges to a point-to-point MIMO link. This generalizes the finite- M result in [33] and shows that the use of relays as active scatterers can recover spatial multiplexing gain in poor scattering environments even if the number of transmit and receive antennas grows large. More importantly, our result shows that linear increase in the number of relays as a function of transmit-receive antennas is sufficient for this to happen. The next step, which is interesting in the context of the MEMBRANE project is to generalize our asymptotic analysis to the multi-hop relaying case, when there exist multiple layers of relays between the source and the destination terminals.

APPENDIX A

SOME ESSENTIALS FROM LARGE RANDOM MATRIX THEORY

In this section, we briefly summarize the basic definitions and results from Large Random Matrix Theory used in this paper. An excellent tutorial on this subject is [35].

Definition 3 (Stieltjes transform): Let $F(x)$ be a distribution function with density $f(x)$. The analytic function

$$G_F(z) \triangleq \int \frac{f(x)}{x-z} dx, \quad z \in \mathbb{C}^+$$

is called the Stieltjes transform of $F(x)$.

Lemma 2 (Inversion formula): Let $G_F(z)$ be the Stieltjes transform of a distribution function $F(x)$. The corresponding density function can be obtained as

$$f(x) = \frac{1}{\pi} \lim_{y \rightarrow 0^+} \Im [G_F(x + jy)]. \quad (47)$$

Theorem 1 (Silverstein [34]): Define the following quantities on a common probability space:

- The random matrix $\mathbf{X} \in \mathbb{C}^{N \times N'}$ has i.i.d. zero-mean entries with variance one.
- The random matrix $\mathbf{Y} \in \mathbb{C}^{N \times N}$ is Hermitian nonnegative definite with $F_{\mathbf{Y}}^N(x)$, for $N \rightarrow \infty$, converging on $[0, \infty)$ a.s. to a nonrandom distribution function $F_{\mathbf{Y}}(x)$ with corresponding density $f_{\mathbf{Y}}(x)$.

Assume that the matrices \mathbf{X} and \mathbf{Y} are statistically independent. Then, for $N, N' \rightarrow \infty$ with $N/N' \rightarrow \beta$, $F_{(1/N')\mathbf{X}\mathbf{X}^H\mathbf{Y}}^N(x) \xrightarrow{\text{a.s.}} F_{(1/N')\mathbf{X}\mathbf{X}^H\mathbf{Y}}(x)$ with its Stieltjes transform $G_{F_{(1/N')\mathbf{X}\mathbf{X}^H\mathbf{Y}}}(z)$ satisfying

$$G_{F_{(1/N')\mathbf{X}\mathbf{X}^H\mathbf{Y}}}(z) = \int_{-\infty}^{\infty} \frac{f_{\mathbf{Y}}(x) dx}{x(1 - \beta - \beta z G_{F_{(1/N')\mathbf{X}\mathbf{X}^H\mathbf{Y}}}(z)) - z}, \quad z \in \mathbb{C}^+. \quad (48)$$

The solution of this fixed-point equation is unique in the set

$$\left\{ G_{F_{(1/N')\mathbf{X}\mathbf{X}^H\mathbf{Y}}}(z) \in \mathbb{C} \mid -\frac{1-\beta}{z} + \beta G_{F_{(1/N')\mathbf{X}\mathbf{X}^H\mathbf{Y}}}(z) \in \mathbb{C}^+ \right\}.$$

We shall furthermore use the Marčenko-Pastur law as stated in [39].

Theorem 2 (Marčenko-Pastur [40]): Assume that the matrix $\mathbf{X} \in \mathbb{C}^{N,N'}$ has i.i.d. zero-mean entries with variance d^2 . Then, for $N, N' \rightarrow \infty$ with $N'/N \rightarrow \beta$, the ESD of $(1/N)\mathbf{X}\mathbf{X}^H$ converges a.s. to a limiting distribution function with density

$$f_{(1/N)\mathbf{X}\mathbf{X}^H}(x) = \frac{\beta}{2\pi x d^2} \sqrt{(\gamma_2 - x)^+ (x - \gamma_1)^+} + [1 - \beta]^+ \delta(x)$$

where $\gamma_1 = d^2(1 - 1/\sqrt{\beta})^2$ and $\gamma_2 = d^2(1 + 1/\sqrt{\beta})^2$.

Under the same assumptions as in the first statement, if, in addition, the entries of \mathbf{X} have finite fourth moments, then a.s.

$$\lim_{N' \rightarrow \infty} \lambda_{\min} \left(\frac{1}{N} \mathbf{X}\mathbf{X}^H \right) = \gamma_1 \quad (49)$$

$$\lim_{N' \rightarrow \infty} \lambda_{\max} \left(\frac{1}{N} \mathbf{X}\mathbf{X}^H \right) = \gamma_2. \quad (50)$$

APPENDIX B

COMPUTATION OF THE INTEGRAL \hat{I} IN (37)

In the following, we detail the computation of the integral

$$\hat{I} \triangleq \rho \int_{\eta_1}^{\eta_2} \frac{\sqrt{(\eta_2 - x)(x - \eta_1)} dx}{x(1-x)^2 \left[x \left(\frac{1-\beta}{z} - \beta G \right) - 1 \right]}$$

on the RHS of (37). With the change of variables

$$t = \sqrt{\frac{x - \eta_1}{\eta_2 - x}}$$

and using the notation

$$\mu_1 \triangleq 1 - \eta_1$$

$$\mu_2 \triangleq 1 - \eta_2$$

$$\nu_1 \triangleq \eta_1 \left(\frac{1-\beta}{z} - \beta G \right) - 1$$

$$\nu_2 \triangleq \eta_2 \left(\frac{1-\beta}{z} - \beta G \right) - 1$$

the integral \hat{I} can be written as

$$\hat{I} = 2(\eta_2 - \eta_1)^2 \rho \int_0^\infty \frac{t^2(t^2 + 1) dt}{(\eta_2 t^2 + \eta_1)(\mu_2 t^2 + \mu_1)^2(\nu_2 t^2 + \nu_1)}.$$

To simplify further, we introduce the notation

$$\kappa_1 \triangleq -\frac{\eta_1}{\eta_2}, \quad \kappa_2 \triangleq -\frac{\mu_1}{\mu_2}, \quad \kappa_3 \triangleq -\frac{\nu_1}{\nu_2}, \quad \chi \triangleq \frac{2(\eta_2 - \eta_1)^2}{\eta_2 \mu_2^2 \nu_2} \rho$$

so that

$$\hat{I} = \chi \int_0^\infty \frac{t^2(t^2 + 1)dt}{(t^2 - \kappa_1)(t^2 - \kappa_2)^2(t^2 - \kappa_3)}. \quad (51)$$

Upon partial fraction expansion of the integrand in (51), we obtain

$$\hat{I} = \chi(A_1 \hat{I}_1 + A_2 \hat{I}_2 + A_3 \hat{I}_3 + A_4 \hat{I}_4)$$

where

$$\begin{aligned} \hat{I}_1 &\triangleq \int_0^\infty \frac{dt}{t^2 - \kappa_1} & \hat{I}_2 &\triangleq \int_0^\infty \frac{dt}{(t^2 - \kappa_2)^2} \\ \hat{I}_3 &\triangleq \int_0^\infty \frac{dt}{t^2 - \kappa_2} & \hat{I}_4 &\triangleq \int_0^\infty \frac{dt}{t^2 - \kappa_3} \end{aligned} \quad (52)$$

with

$$A_1 = \frac{\kappa_1(\kappa_1 + 1)}{(\kappa_1 - \kappa_2)^2(\kappa_1 - \kappa_3)} \quad (53)$$

$$A_2 = \frac{\kappa_2(\kappa_2 + 1)}{(\kappa_2 - \kappa_1)(\kappa_2 - \kappa_3)} \quad (54)$$

$$A_3 = \frac{-\kappa_2^2 - \kappa_1\kappa_2^2 + \kappa_1\kappa_3 + 2\kappa_1\kappa_2\kappa_3 - \kappa_2^2\kappa_3}{(\kappa_2 - \kappa_1)^2(\kappa_2 - \kappa_3)^2} \quad (55)$$

$$A_4 = \frac{\kappa_3(\kappa_3 + 1)}{(\kappa_3 - \kappa_1)(\kappa_3 - \kappa_2)^2}. \quad (56)$$

The integrals in (52) can be evaluated resulting in

$$\hat{I}_1 = \frac{1}{\sqrt{-\kappa_1}} \arctan \frac{t}{\sqrt{-\kappa_1}} \Big|_0^\infty = \frac{\pi}{2\sqrt{-\kappa_1}} \quad (57)$$

$$\hat{I}_2 = -\frac{t}{2\kappa_2(t^2 - \kappa_2)} \Big|_0^\infty - \frac{1}{2\kappa_2\sqrt{-\kappa_2}} \arctan \frac{t}{\sqrt{-\kappa_2}} \Big|_0^\infty = -\frac{\pi}{4\kappa_2\sqrt{-\kappa_2}} \quad (58)$$

$$\hat{I}_3 = \frac{1}{\sqrt{-\kappa_2}} \arctan \frac{t}{\sqrt{-\kappa_2}} \Big|_0^\infty = \frac{\pi}{2\sqrt{-\kappa_2}} \quad (59)$$

$$\hat{I}_4 = \frac{1}{\sqrt{-\kappa_3}} \arctan \frac{t}{\sqrt{-\kappa_3}} \Big|_0^\infty = \frac{\pi}{2\sqrt{-\kappa_3}}. \quad (60)$$

The quantity κ_3 is complex-valued and the arctan and square root in (59) are understood as the principal values of these functions in \mathbb{C} as defined in [41].

Finally, by inspection, combining (57)–(60) with (53)–(56) and resubstituting the values of the parameters $\kappa_1, \kappa_2, \kappa_3, \chi, \rho, \mu_1, \mu_2, \eta_1, \eta_2, \nu_1, \nu_2, \gamma_1$, and γ_2 , after straightforward but tedious simplifications, we find

$$\chi A_1 \hat{I}_1 = \frac{(\sqrt{\beta} + 1) |\sqrt{\beta} - 1|}{2\beta} \quad (61)$$

$$\chi A_2 \hat{I}_2 = -\frac{z}{\sqrt{\beta}(G\beta z + z + \beta - 1)} \quad (62)$$

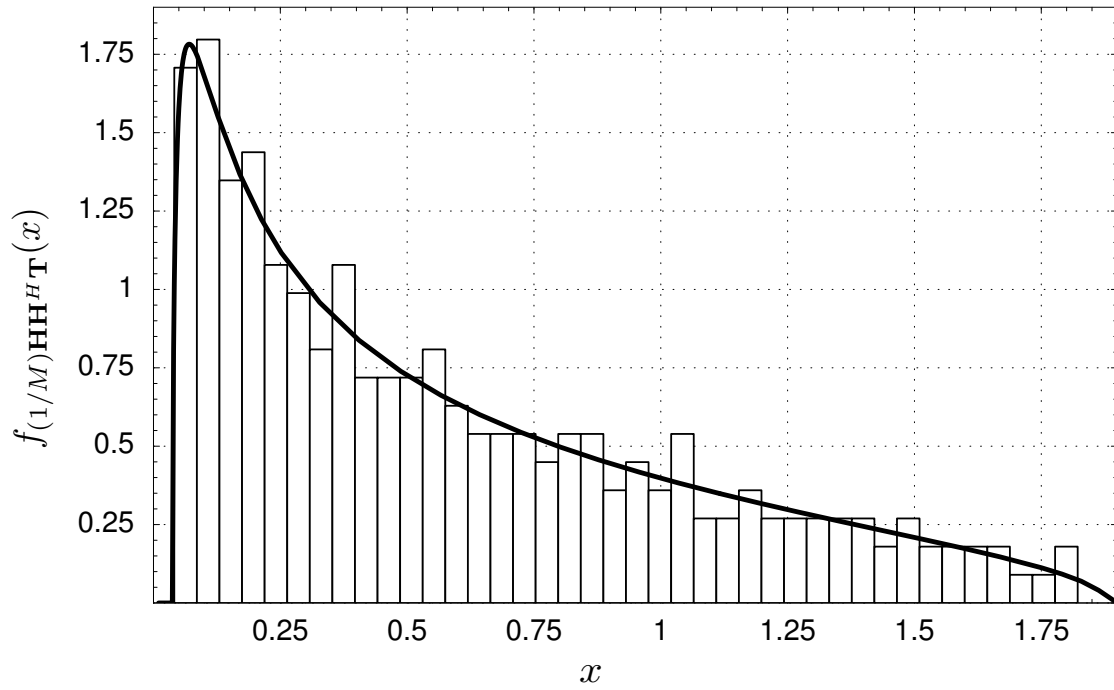
$$\chi A_3 \hat{I}_3 = -\frac{z \left(d^2 (\sqrt{\beta} - 1)^2 (G\beta z + z + \beta - 1) - \beta(G\beta z + \beta - 1) \right)}{2d^2 \beta (G\beta z + z + \beta - 1)^2} \quad (63)$$

$$\chi A_4 \hat{I}_4 = -\frac{(G\beta z + \beta - 1) \sqrt{\frac{d^2 (G\beta z + z + \beta - 1) (\sqrt{\beta} - 1)^2 + z\beta}{d^2 (G\beta z + z + \beta - 1) (\sqrt{\beta} + 1)^2 + z\beta}}}{2d^2 \beta (G\beta z + z + \beta - 1)^2} \left(d^2 (G\beta z + z + \beta - 1) (\sqrt{\beta} + 1)^2 + z\beta \right). \quad (64)$$

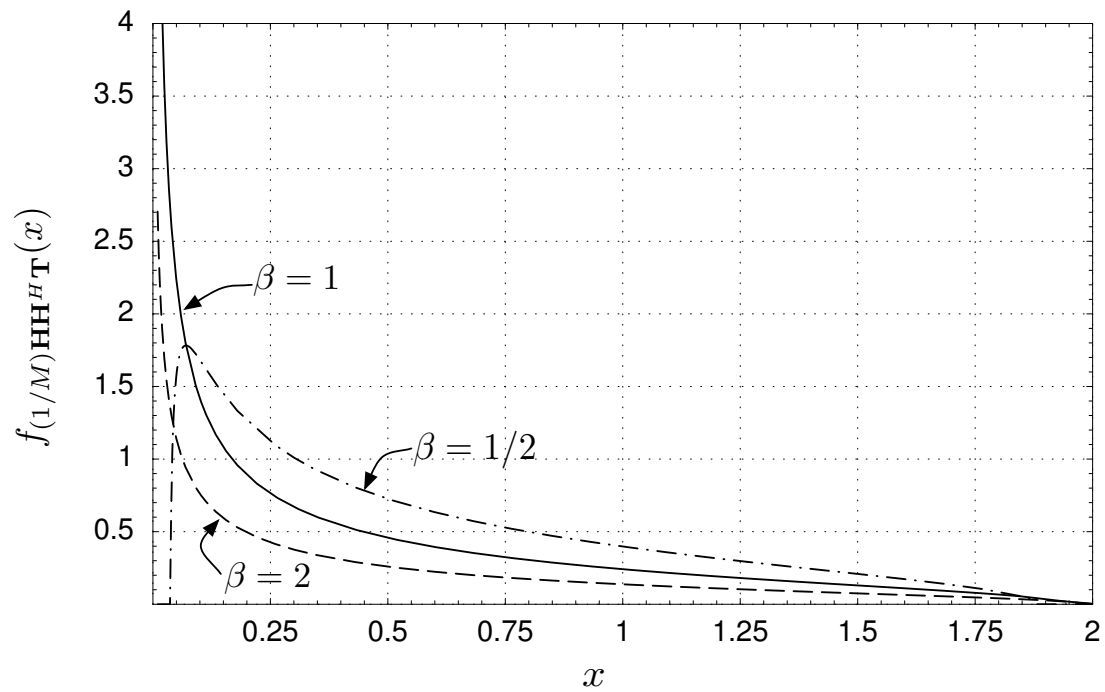
REFERENCES

- [1] E. C. van der Meulen, “Three-terminal communication channels,” *Adv. Appl. Prob.*, vol. 3, pp. 120–154, 1971.
- [2] T. M. Cover and A. E. Gamal, “Capacity theorems for the relay channel,” *IEEE Trans. Inf. Theory*, vol. 25, no. 5, pp. 572–584, Sept. 1979.
- [3] J. Guey, M. P. Fitz, M. R. Bell, and W. Kuo, “Signal design for transmitter diversity wireless communication systems over Rayleigh fading channels,” in *Proc. IEEE VTC*, vol. 1, Atlanta, GA, Apr./May 1996, pp. 136–140.
- [4] V. Tarokh, N. Seshadri, and A. R. Calderbank, “Space-time codes for high data rate wireless communication: Performance criterion and code construction,” *IEEE Trans. Inf. Theory*, vol. 44, no. 2, pp. 744–765, March 1998.
- [5] S. M. Alamouti, “A simple transmit diversity technique for wireless communications,” *IEEE J. Sel. Areas Comm.*, vol. 16, no. 8, pp. 1451–1458, Oct. 1998.
- [6] V. Tarokh, H. Jafarkhani, and A. Calderbank, “Space-time block codes from orthogonal designs,” *IEEE Trans. Inf. Theory*, vol. 45, no. 5, pp. 1456–1467, July 1999.
- [7] A. Sendonaris, E. Erkip, and B. Aazhang, “User cooperation diversity – Part I: System description,” *IEEE Trans. Comm.*, vol. 51, no. 11, pp. 1927 – 1938, Nov. 2003.
- [8] —, “User cooperation diversity – Part II: Implementation aspects and performance analysis,” *IEEE Trans. Comm.*, vol. 51, no. 11, pp. 1939 – 1948, Nov. 2003.
- [9] J. N. Laneman, G. W. Wornell, and D. N. C. Tse, “An efficient protocol for realizing cooperative diversity in wireless networks,” in *Proc. IEEE ISIT*, Washington, DC, June 2001, p. 294.
- [10] J. N. Laneman, D. N. C. Tse, and G. W. Wornell, “Cooperative diversity in wireless networks: Efficient protocols and outage behavior,” *IEEE Trans. Inf. Theory*, to appear.
- [11] J. N. Laneman and G. W. Wornell, “Energy-efficient antenna sharing and relaying for wireless networks,” in *Proc. IEEE WCNC*, vol. 1, Chicago, IL, Sept. 2000, pp. 7–12.
- [12] A. Stefanov and E. Erkip, “Cooperative coding for wireless networks,” in *Proc. Int. Workshop on Mobile and Wireless Comm. Networks*, Stockholm, Sweden, Sept. 2002, pp. 273–277.
- [13] T. E. Hunter and A. Nosratinia, “Cooperative diversity through coding,” in *Proc. IEEE ISIT*, Lausanne, Switzerland, June 2002, p. 220.
- [14] A. Host-Madsen, “On the capacity of wireless relaying,” in *Proc. IEEE VTC*, vol. 3, Vancouver, Canada, Sept. 2002, pp. 1333–1337.
- [15] J. N. Laneman and G. W. Wornell, “Distributed space-time-coded protocols for exploiting cooperative diversity in wireless networks,” *IEEE Trans. Inf. Theory*, vol. 49, no. 10, pp. 2415 – 2425, Oct. 2003.

- [16] R. U. Nabar, H. Bölcskei, and F. W. Kneubühler, "Fading relay channels: Performance limits and space-time signal design," *IEEE J. Sel. Areas Comm.*, 2004, to appear.
- [17] K. Azarian, H. E. Gamal, and P. Schniter, "On the achievable diversity-multiplexing tradeoff in half-duplex cooperative channels," *IEEE Trans. Inf. Theory*, vol. 51, no. 12, pp. 4152–4172, December 2005.
- [18] S. Yang and J.-C. Belfiore, "Towards the optimal amplify-and-forward cooperative diversity scheme," *IEEE Transactions on Information Theory*, 2007.
- [19] R. Mudumbai, J. Hespanha, U. Madhow, and G. Barriac, "Distributed transmit beamforming using feedback control," *Preprint*.
- [20] R. Mudumbai, G. Barriac, and U. Madhow, "On the feasibility of distributed beamforming in wireless networks," *Preprint*.
- [21] H. Ochiai, P. Mitran, H. V. Poor, and V. Tarokh, "Collaborative beamforming for distributed wireless ad hoc sensor networks," *Preprint*.
- [22] R. Ahlswede, N. Cai, S. Y. R. Li, and R. W. Yeung, "Network information flow," *IEEE Trans. Inf. Theory*, vol. 46, pp. 1204–1216, July 2000.
- [23] N. Cai and R. W. Yeung, "Secure network coding," in *Proc. IEEE ISIT*, Lausanne, Switzerland, June 2002, p. 323.
- [24] R. Koetter and M. Medard, "An algebraic approach to network coding," *IEEE/ACM Trans. on Networking*, vol. 11, no. 5, pp. 782–795, Oct. 2003.
- [25] A. J. Paulraj and T. Kailath, "Increasing capacity in wireless broadcast systems using distributed transmission/directional reception," *U. S. Patent*, no. 5,345,599, 1994.
- [26] G. J. Foschini, "Layered space-time architecture for wireless communication in a fading environment when using multi-element antennas," *Bell Labs Tech. J.*, pp. 41–59, 1996.
- [27] I. E. Telatar, "Capacity of multi-antenna Gaussian channels," *European Trans. Tel.*, vol. 10, no. 6, pp. 585–595, Nov./Dec. 1999.
- [28] H. Bölcskei, D. Gesbert, and A. J. Paulraj, "On the capacity of OFDM-based spatial multiplexing systems," *IEEE Trans. Comm.*, vol. 50, no. 2, pp. 225–234, Feb. 2002.
- [29] L. H. Ozarow, S. Shamai, and A. D. Wyner, "Information theoretic considerations for cellular mobile radio," *IEEE Trans. Veh. Technol.*, vol. 43, no. 2, pp. 359–378, May 1994.
- [30] E. Biglieri, J. Proakis, and S. Shamai, "Fading channels: Information-theoretic and communications aspects," *IEEE Trans. Inf. Theory*, vol. 44, no. 6, pp. 2619–2692, Oct. 1998.
- [31] L. Zheng and D. N. C. Tse, "Diversity and multiplexing: A fundamental tradeoff in multiple-antenna channels," *IEEE Trans. Inf. Theory*, vol. 49, no. 5, pp. 1073–1096, May 2003.
- [32] A. Carleial, "Interference channels," *IEEE Trans. Inf. Theory*, vol. 24, no. 1, pp. 60–71, Jan. 1978.
- [33] H. Bölcskei, R. U. Nabar, Ö. Oyman, and A. J. Paulraj, "Capacity scaling laws in MIMO relay networks," *IEEE Trans. Wireless Commun.*, vol. 5, no. 6, pp. 1433 – 1444, June 2006.
- [34] J. W. Silverstein, "Strong convergence of the empirical distribution of eigenvalues of large dimensional random matrices," *J. Multivariate Anal.*, vol. 55, pp. 331–339, Nov. 1995.
- [35] A. M. Tulino and S. Verdú, "Random matrix theory and wireless communications," *Foundations and Trends in Communications and Information Theory*, vol. 1, no. 1, pp. 1–182, 2004.
- [36] R. R. Müller, "Applications of large random matrices in communications engineering," in *Proc. of International Conference on Advances in the Internet, Processing, Systems, and Interdisciplinary Research (IPSI)*, Sveti Stefan, Montenegro, Oct. 2003.
- [37] R. U. Nabar and H. Bölcskei, "Capacity scaling laws in asynchronous relay networks," in *Proc. Allerton Conf. Commun., Contr., Comput.*, Oct. 2004.
- [38] I. E. Telatar, "Capacity of multi-antenna Gaussian channels," *Eur. Trans. Telecommun.*, vol. 10, no. 6, pp. 585–595, Nov. 1999.
- [39] Z. D. Bai, "Methodologies in spectral analysis of large dimensional random matrices," *Statistica Sinica*, vol. 9, pp. 611–677, 1999.
- [40] V. A. Marčenko and L. A. Pastur, "Distribution of some sets of random matrices," *Math. USSR-Sb.*, vol. 1, pp. 457–483, 1967.
- [41] M. Abramowitz and I. A. Stegun, *Handbook of Mathematical Functions*. Dover Publications, 1964.



(a)



(b)

Fig. 7. Limiting density $f_{(1/M)HH^HT}(x)$ (a) for $\beta = 1/2$ and $d = 1$ along with its histogram (Monte-Carlo) and (b) for different values of $\beta = 2, 1, 1/2$ and $d = 1$.

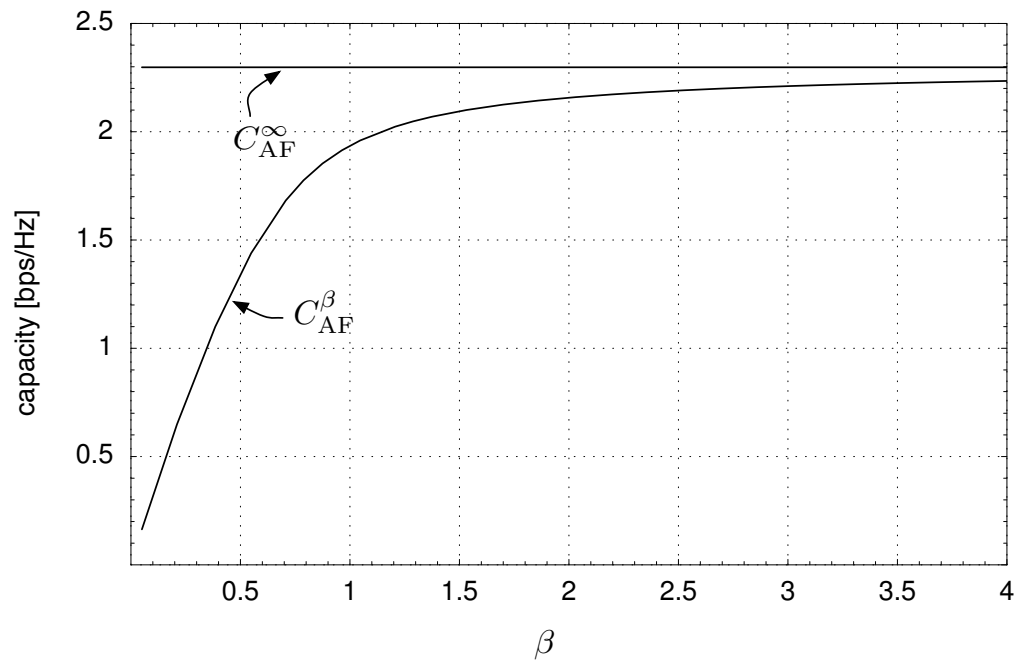


Fig. 8. Capacity C_{AF}^{β} as a function of β for $d = 1$ and $\sigma^2 = 0.01$.